Strojniški vestnik - Journal of Mechanical Engineering 56(2010)6, 409-417 Paper received: 19.09.2008
UDC UDK 629.4.027.31-272.2:531.2:004.8 Paper accepted: 16.04.2010

Application of Artificial Neural Networks in the Prediction of Critical Buckling Loads of Helical Compression Springs

Turgay Ibrikçi[1,*] - Selim Saçma[2] - Vebil Yıldırım[2] - Tarkan Koca[3]

[1]Çukurova University, Electrical-Electronics Engineering Department, Turkey
[2]Çukurova University, Mechanical Engineering Department, Turkey
[3]University of İnönü, Arapgir Vocational School, Turkey

This paper proposes the use of artificial neural networks (ANN) to perfectly predict the critical buckling loads of cylindrical isotropic helical spring with fixed ends and with circular sections, and with large pitch angles. The buckling equations of cylindrical isotropic helical springs loaded axially consist of a set of twelve linear differential equations. As finding a solution in an analytical manner is too difficult, numerical solution in an exact manner based on the transfer-matrix method to collect consistent dimensionless numerical data for the training process is used. In this way almost perfect weight values are obtained to predict the non-dimensional buckling loads. A good agreement is observed with the data available in the literature.

Keywords: buckling, critical buckling load, helical spring, artificial neural networks, design, coil spring

0 INTRODUCTION

As helical springs are an essential element of mechanisms and machines, they are widely used in numerous engineering applications. By means of developed analytical formulas based on the small helix pitch angle assumptions that are available in mechanical engineering text books, the design of such a helical spring is generally performed by the method of trial and error or by using design charts.

The pioneering author Haringx [1] presented a buckling formula in a closed form for cylindrical helical springs, with the use of a rod-model approximation. For the buckling behavior of the helical springs with large helix pitch angles a few numerical studies have been undertaken [2] to [10]. The finite element method [2] to [4] and the transfer matrix method [5] to [10] are generally preferred in the numerical solution process. Those studies have shown that Haringx's [1] formula gives accurate results only when the helical spring has a small helix pitch angle. Chassie et al. [9] have also presented some reliable buckling charts to be used in the design stage of cylindrical helical isotropic compression springs with clamped ends and with circular sections. In the numerical works associated with the buckling behavior of the helical springs with large pitch angles as mentioned above, the effect of both axial and shear deformations are considered [2] to [10]. It may be noted that in references [2] to [9], only the contribution of the torsional moment on the axial deflection is considered. As expected, for large helix pitch angles the effects of axial and shearing forces together with the bending moment should also be taken into account in order to achieve a complete formulation of the problem to as in the present work[10].

In the first part of the current work, the buckling behavior of isotropic cylindrical compression helical springs subjected to an axial static force and with a circular section is examined in a static manner by using both the buckling equations given by Yıldırım and the buckled deformation equations presented by Yıldırım [10]. The transfer matrix method is used for the numerical analysis. To obtain an exact numerical overall transfer matrix of the spring an effective numerical algorithm available in the literature [11] is also employed. The axial and shear deformation effects are all considered based on the first order shear deformation theory. For the determination of the vertical deflection of the springs with large pitch angles, analytical expressions, which are obtained based on Castigliano's first theorem, are used to take into

*Corr. Author's Address : Cukurova University Electrical-Electronics Dept. 01330 Adana Turkey
ibrikci@cukurova.edu.tr

account the effect of the whole stress resultants such as axial and shearing forces, bending and torsional moments on the tip deflection.

For the training process in ANN, in the second part of the present study, some exact numerical dimensionless buckling load data are collected by choosing the main parameters of the spring within a large range that affect the buckling behavior. An ANN procedure with almost perfect weight values is proposed to predict the buckling loads to be used directly in the design stage of the helical springs.

1 DIFFERENTIAL BUCKLING EQUATIONS OF A CYLINDRICAL HELICAL SPRING SUBJECTED TO AN AXIAL STATIC FORCE

Consider a spatial bar. Let *s* be curvilinear position coordinate (Fig. 1). Let $T(s)=(T_t, T_n, T_b)$ be the internal force vector, and let $M(s)=(M_t, M_n, M_b)$ be the internal moment vector, where T_t is the axial force; T_n and T_b are the shearing forces; M_t is the torsional moment; and M_n and M_b are the bending moments, respectively. Let $\Omega(s)=(\Omega_t, \Omega_n, \Omega_b)$ be the rotation vector, and $U(s)=(U_t, U_n, U_b)$ be the displacement vector in Frenet coordinates (*t,n,b*). Initial internal static force and moment vectors are denoted by $T^o(s)$ and $M^o(s)$, respectively.

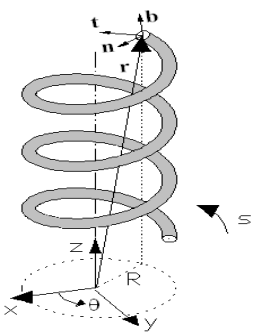

Fig. 1. *Frenet coordinates*

Yıldırım [10] derived the following buckling equation set in a vector form for a spatial bar:

$$\frac{dU}{ds} - \Theta_T T + t \times \Omega = 0, \qquad (1a)$$

$$\frac{d\Omega}{ds} - \Theta_M M = 0, \qquad (1b)$$

$$\frac{dT}{ds} + (\Theta_M M) \times T^o = 0, \qquad (1c)$$

$$\frac{dM}{ds} + (\Theta_M M) \times M^o + t \times T + (\Theta_T T) \times T^o = 0. \qquad (1d)$$

For isotropic bar material and doubly symmetric sections

$$\Theta_T = \begin{bmatrix} \frac{1}{EA} & 0 & 0 \\ 0 & \frac{k}{GA} & 0 \\ 0 & 0 & \frac{k}{GA} \end{bmatrix}, \qquad (2a)$$

$$\Theta_M = \begin{bmatrix} \frac{1}{GJ_b} & 0 & 0 \\ 0 & \frac{1}{EI_n} & 0 \\ 0 & 0 & \frac{1}{EI_b} \end{bmatrix}. \qquad (2b)$$

In the above, the undeformed cross-sectional area is denoted by *A,* the moments of inertia with respect to the normal and binormal axes are denoted by I_n and I_b, respectively. J_b is the torsional moment of inertia, *G* is the shear modulus and *E* is the Young's modulus. *k* represents the Timoshenko's *k*-factors.

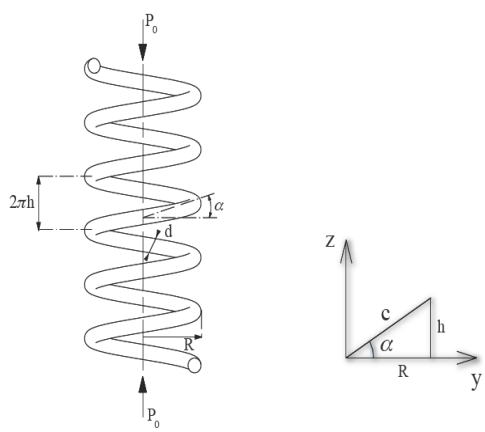

Fig. 2. *Geometry of a helix subjected to an axial compressive force*

Let α be the helix pitch angle, θ be the angular coordinate, and *R = (D/2)* be the radius of the cylinder (Fig. 2). Frenet-Serret relations for cylindrical helical springs are given by

$$\frac{dt}{ds} = \chi\, n = \frac{R}{c^2}\, n \qquad (3a)$$

$$\frac{dn}{ds} = \tau\, b - \chi\, t = \frac{h}{c^2}\, b - \frac{R}{c^2}\, t, \qquad (3b)$$

$$\frac{db}{ds} = -\tau\, n = -\frac{h}{c^2}\, n, \qquad (3c)$$

where χ is the curvature and τ is the tortuosity of the helix. The infinitesimal arc length of the spring, *ds*, is obtained as follows:

$$ds = cd\theta = \frac{R}{\cos\alpha} d\theta . \qquad (4)$$

The free axial length of the helix is defined by

$$\frac{L_0}{D} = n\pi \tan\alpha , \qquad (5)$$

where the total number of active turns is denoted by *n*. The Frenet components of the initial force and moment vectors will be in the following form of (Fig. 2):

$$T^o = (-P_o \sin\alpha, 0, -P_0 \cos\alpha), \qquad (6a)$$

$$M^o = (-P_o R\cos\alpha, 0, P_0 R\sin\alpha). \qquad (6b)$$

Using Eqs (2 to 4), (6) and (1), a set of twelve linear differential scalar equations in Frenet trihedral, which govern the buckling of the cylindrical helical springs subjected to an axial static force, are written as follows:

$$\frac{dU_t}{d\theta} = \cos\alpha U_n + \frac{1}{EA} T_t , \qquad (7a)$$

$$\frac{dU_n}{d\theta} = -\cos\alpha U_t + \sin\alpha U_b + \frac{R}{\cos\alpha}\Omega_b + \frac{kR}{GA\cos\alpha} T_n , \qquad (7b)$$

$$\frac{dU_b}{d\theta} = -\sin\alpha U_n - \frac{R}{\cos\alpha}\Omega_n + \frac{kR}{GA\cos\alpha} T_b , \qquad (7c)$$

$$\frac{d\Omega_t}{d\theta} = \cos\alpha\Omega_n + \frac{R}{GJ_b\cos\alpha} M_t , \qquad (7d)$$

$$\frac{d\Omega_n}{d\theta} = -\cos\alpha\Omega_t + \sin\alpha\Omega_b + \frac{R}{EI_n\cos\alpha} M_n , \qquad (7e)$$

$$\frac{d\Omega_b}{d\theta} = -\sin\alpha\Omega_n + \frac{R}{EI_b\cos\alpha} M_b , \qquad (7f)$$

$$\frac{dT_t}{d\theta} = \cos\alpha T_n + \frac{P_o R}{EI_n} M_n , \qquad (7g)$$

$$\frac{dT_n}{d\theta} = -\cos\alpha T_t + \sin\alpha T_b - \frac{P_o R}{GJ_b} M_t + \frac{P_o R\tan\alpha}{EI_b} M_b , \qquad (7h)$$

$$\frac{dT_b}{d\theta} = -\sin\alpha T_n - \frac{P_o R\tan\alpha}{EI_n} M_n , \qquad (7i)$$

$$\frac{dM_t}{d\theta} = \frac{kP_o R}{GA} T_n + (\cos\alpha - \frac{P_o R^2\tan\alpha}{EI_n}) M_n , \qquad (7j)$$

$$\frac{dM_n}{d\theta} = -\frac{P_o R}{EA} T_t + (\frac{R}{\cos\alpha} + \frac{kP_o R\tan\alpha}{GA}) T_b + + (-\cos\alpha + \frac{P_o R^2\tan\alpha}{GJ_b}) M_t + (\sin\alpha + \frac{P_o R^2}{EI_b}) M_b , \qquad (7k)$$

$$\frac{dM_b}{d\theta} = -(\frac{kP_o R\tan\alpha}{GA} + \frac{R}{\cos\alpha}) T_n - -(\sin\alpha + \frac{P_o R^2}{EI_n}) M_n . \qquad (7l)$$

These linear differential equations with constant coefficients are valid for isotropic cylindrical helical springs with constant sections having double symmetry axes such as circle, rectangle etc. The first terms of Eqs. (7*j*), (7*k*) and (7*l*) are the major contribution of Yıldırım [10] to the literature. These equations are solved numerically with the help of the transfer matrix method and the numerical algorithm developed by Yıldırım [11].

To determine the buckled deformations, Yıldırım [10] derived analytical expressions for the vertical tip deflection of helical springs with large pitch angles and an arbitrary shape by taking into account for the whole effect of the stress resultants such as axial and shearing forces, bending and torsional moments with the use of Castigliano's first theorem. For cylindrical isotropic helical springs with circular cross-sections, the following formulas are used for the determination of the vertical tip deflection [10]:

$$\delta_{T_b} = \frac{332.8 P_0 Rn\cos\alpha}{Gd^4} , \qquad (8a)$$

$$\delta_{T_t} = \frac{20.8 P_0 Rn\sin\alpha\cos\alpha}{Gd^2} , \qquad (8b)$$

$$\delta_{M_b} = \frac{128 P_0 R^3 n\sin\alpha\cos\alpha}{Gd^4} , \qquad (8c)$$

$$\delta_{M_t} = \frac{64 P_0 nR^3\cos\alpha}{Gd^4} , \qquad (8d)$$

$$\delta_{Total} = \delta_{T_t} + \delta_{T_b} + \delta_{M_t} + \delta_{M_b} . \qquad (8e)$$

Eq. (8*d*) takes into account of just the effect of the torsional moment on the tip deflection. For quick insight, percent contributions of both the bending and torsional moment on the vertical deflection are illustrated in Fig. 3. As seen from Fig. 3 for $\alpha = 40^o$ the percent contribution of the torsional moment on the total vertical deflection decreases to 65%, while this contribution reaches over 95% for $\alpha = 10^o$.

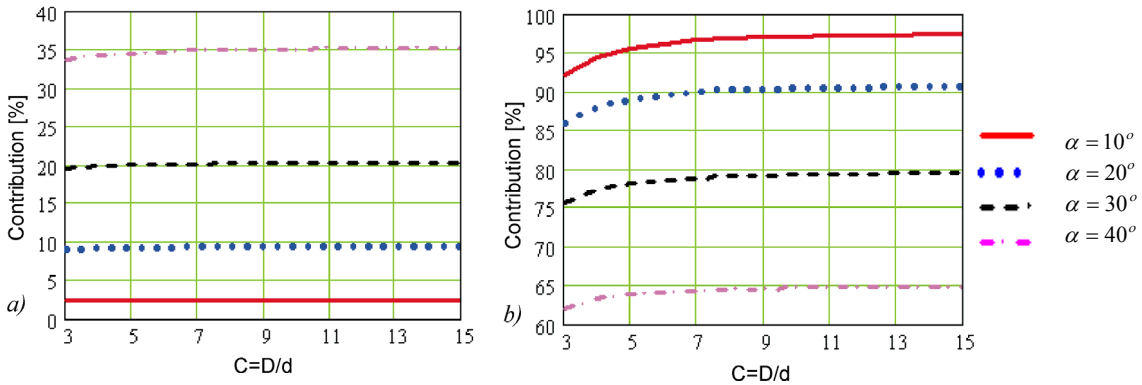

Fig. 3. *Percent contributions of a) bending moment b) torsional moment on the total axial deflection of a cylindrical isotropic spring with circular section [11] (d = 1.85 cm, G = 800000kg$_f$/cm^2, P = 150 kg$_f$ n = 18, ν = 0.3, k = 1.1)*

It may be noted that these effects gain considerable importance for especially rectangular cross-sections. Consequently the true computation of the buckled deformation of the spring under a static axial force is one of the crucial steps of the buckling analysis.

The application of Artificial Neural Networks in mechanical engineering problems has become increasingly known in recent years. Therefore, this approach was specifically applied in the field of "critical buckling loads of helical compression springs".

2 ARTIFICIAL NEURAL NETWORKS

Artificial Neural Networks (ANN) are models of a highly parallel and adaptive computation based on very loose simulations of the brain [12]. In fact, there is no universally accepted definition of neural networks. It is a network with simple processors which are called "units, nodes or PE-Processing units", with a small local memory. These processor units are usually organized in a sequence of layers. Typically, an ANN contains two or more layers; the first layer is called the input layer where data is presented to the network. An output layer is the interface of the outside of network; the output layer presents the result of the network. In the inside of the networks, between the input and output layer, there is a layer called the hidden layer. Each node in a layer is connected to other nodes with connections called weights. A node sums the weighted input, and uses one activation function, and sends an output to the nodes to which it is connected. In general, there are two types of learning with ANN which are supervised and unsupervised. In supervised learning, the ANN learns on a training example set which consists of many pairs of input/output (I/O) mapping forms of the training examples. The network is trained by a training set in unsupervised learning and there is no input/output mapping of the training set that consists of input training examples only. There is no teacher learning as the network learns to adapt based on training examples.

A node structure is shown in Fig. 4. The node is the basic information processing unit of an ANN. It consists of:

i) a set of connections, describing the node inputs X = { x_i, x_{i+1}, x_{i+2} ..., x_n} with weights W = {w_i, w_{i+1}, w_{i+2} ..., w_n},

ii) a summing function, for finding the weighted sum of the inputs with bias,

$$u = \mathrm{X}\mathrm{W}^T \text{ or } u = \sum_{i=1}^{n} w_i x_i + b \tag{9}$$

iii) an activation function-sigmoid function for squeezing of the output.

$$y = \varphi(u) = \frac{1}{1+e^{-u}} \tag{10}$$

where y is the output of the network between 0 and 1.

Backpropagation (BP) [13] networks as one of the supervised ANN methods may provide answers in many different fields such as machine learning, and engineering problems [14] and [15]. A BP network consists of at least three layers: an input layer, at least one hidden layer, and an output layer. BP learns by iteratively processing a set of training examples. When a BP network is

cycled, an input example is propagated forward to the output through the intervening input-to-hidden and hidden-to-output weights.

3 THE PROPOSED ARTIFICIAL NEURAL NETWORK SYSTEM

In this study, the three layers – BP algorithm is applied to calculate the best estimation of the critical buckling loads of isotropic cylindrical helical springs subjected to an axial static force (Fig. 5).

The spring with clamped ends is assumed to have a circular cross-section. Exact numerical critical buckling loads are obtained numerically by solving a set of linear differential equations in Eq. set (7). +Some numerical data calculated in such a way is used to determine the optimum weights and the desired BP algorithm to predict the critical dimensionless buckling loads determined by Eq. (11).

$$\overline{P}_{cr} = \frac{R^2}{EI_n \cos^2 \alpha_0} P \cdot \tag{11}$$

The ratio of the mean coil diameter to wire diameter is referred to the spring index.

$$C = \frac{D}{d} = \frac{D_0}{d} \ . \tag{12}$$

The spring index, C, the total number of active coils, n, and the ratio of L_0/D_0 are being independent values of inputs X.

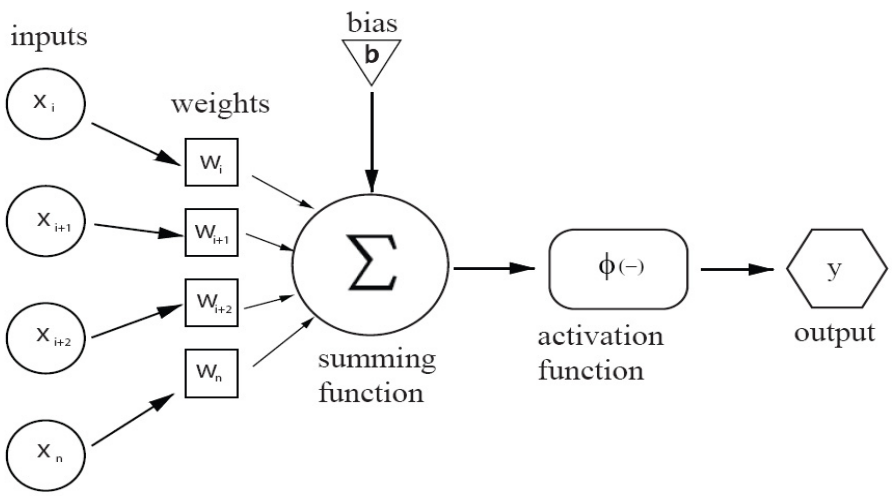

Fig. 4. *A simple node structure*

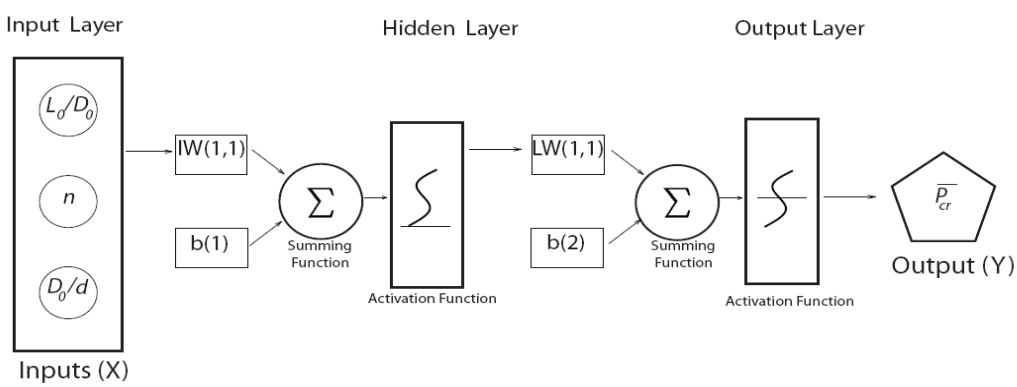

Fig. 5. *The structure of the proposed ANN*

MATLAB Neural Network Toolbox is used for BP calculations [16]. The first step of this research is to normalize the data. In order to squeeze *X* values and output between *0* and *1*, a normalization process is applied. The normalization equation which performs a linear transformation of the original data is

$$X_n = (X_{\max} - X_{\min}) \times \frac{(X - X_{\min})}{(X_{\max} - X_{\min})} - X_{\min} \tag{13}$$

where X_{min} and X_{max} respectively are the minimum and maximum values in the data X. After the normalization of the data at the second stage of the reach, The Matlab functions were used for "training" and "testing". The training data set has *3662* patterns values (Table 1) for training the network for about 5000 epochs. For training, the "*Trainlm*" training function is used, which is a network training function that updates weights and bias values according to the *Levenberg-Marquardt (LM)* optimization which is the most widely used optimization algorithm[15]. It outperforms simple gradient descent and other conjugate gradient methods in a wide variety of problems. Another function that can be used is *"Learngdm"* function which is the gradient descent with momentum weight and bias learning functions. The "mse" function is used as "Network Performance Function" which measures the network's performance according to the mean of squared errors with Eq. (14) [16]. The Eq. could be written

$$E = \frac{1}{n} \sum_{i=1}^{n} \left\| o_i - t_i \right\|^2, \tag{14}$$

where the *o* and *t* are the output, and the desired output respectively. The *W* and *b* values will be updated until the epoch number is reached.

The relative error is determined as:

$$RE(\%) = \left\{ \frac{P_{cr}^{(ANN)} - P_{cr}^{(NUMERICAL)}}{P_{cr}^{(NUMERICAL)}} \right\} 100, \tag{15}$$

where $P_{cr}^{(ANN)}$ is a calculated value of the critical buckling load by ANN, and $P_{cr}^{(NUMERICAL)}$ is a numerical value of the critical buckling load by using the Eq. set (7).

The ANNs results are tested with the testing set given in Table 2 which consists of a total 1305 numerical critical buckling loads. In this test, the distinct maximum relative error for dimensionless critical buckling loads is found as 0.93%.

4 NUMERICAL EXAMPLES

To verify the numerical results obtained by the present study, some benchmark results in the available literature were also considered in this section. Apart from this, some design charts are presented by using the ANN data. The Young's modulus and Poisson's ratio of the benchmark spring material with fixed ends are $E = 210$ *GPa* and $\upsilon = 0.3$, respectively. Geometrical properties of the benchmark springs are presented in Table 3. Table 4 shows the comparison of the present results with the benchmark studies available in the literature. Graphs in Figs. 6 and 7 illustrate the comparison of the present numerical (exact) and ANN dimensional critical buckling loads for a different number of active turns and spring indices.

Table 4 shows a good agreement between the data results obtained so far. As seen from the table, the present numerical results, in general, are between the results in references [3] and [9]. While Tabarrok and Xiong [3] have used the finite element procedure, Chassie et al. [9] have preferred the transfer matrix approach as in the present study. For large L_0/D_0 ratios, Haringx's [1] analytical results give greater critical buckling loads than all the numerical results in Table 4. The proposed ANN results are very close to the numerical results in the present work. As stated above, the distinct maximum relative error for dimensionless critical buckling loads in the questioning set given by Table 2 is found as 0.93%. It may be concluded that the critical buckling loads with ANN may be accepted as satisfactory even for the buckling loads that are out of the range of the training data set. Therefore, the ANN method proposed in this paper may be used for the consistent design of any spring.

5 CONCLUSIONS

In this study artificial neural networks (ANN) are used to predict the critical buckling loads of cylindrical isotropic helical springs with fixed ends and with circular sections, and with large-pitch angles together with the numerical solution of the differential equation set governing the buckling behavior of such springs.

Table 1. *The training data set*

C	*N*	*Number of taken values*	*C*	*n*	*Number of taken values*	*C*	*n*	*Number of taken values*
7	5	36	9	5	36	11	5	36
	7	36		7	36		7	36
	9	36		9	36		9	36
	10	36		10	36		10	36
	11	36		11	36		11	36
	13	36		13	36		13	36
	15	36		15	36		15	36
	17	36		17	36		17	33
	19	36		19	33		19	31
	20	36		20	32		20	28
	21	36		21	32		21	28
	23	34		23	31		23	22
	25	34		25	20		25	16
	29	27		29	14		29	11
	30	22		30	17		30	10
6	5	107	8	5	107	10	5	107
	10	108		10	108		10	108
	15	108		15	108		15	108
	20	108		20	108		20	94
	25	105		25	79		25	65
	30	85		30	52		30	50
12	5	107	*Total = 3662 patterns*					
	10	108						
	15	107						
	20	73						
	25	48						
	30	27						

Table 2. *The testing data set*

C	*N*	*Number of taken values*	*C*	*N*	*Number of taken values*	*C*	*n*	*Number of taken values*
6.5	5	36	7.5	5	36	8.5	5	36
	9	36		9	36		9	36
	13	36		13	36		13	36
	17	36		17	36		17	36
	21	36		21	34		21	32
	25	35		25	31		25	30
	29	26		29	24		29	18
9.5	5	36	10.5	5	36	11.5	5	36
	9	36		9	36		9	36
	13	36		13	36		13	36
	17	36		17	34		17	33
	21	29		21	26		21	27
	25	20		25	19		25	18
	29	13		29	14		29	14
Total = 1305 patterns								

Table 3. *Geometrical properties of the benchmark springs*

Spring number	L_o [mm]	D_o [mm]	$\frac{L_0}{D_0}$	D [mm]	$C=\frac{D_0}{d}$	n	$\alpha_0\,(^o)$
1	240	40	6	8	5	6	17.657
2	720	100	7.2	25	4	15	8.687
3	90	10	9	4	2.5	15	10.812
4	120	10	12	2	5	20	10.812
5	240	20	12	4	5	6	32.482

Table 4. *Comparison of the critical dimensionless buckling loads*

Spring number	$\alpha_{cr}\,(^o)$	Tabarrok and Xiong [3]	Chassie et al [9]	Haringx [1]	Present Study		
					Numerical	ANN	Relative error (%)
1	10.1800	0.1061	0.1200	0.1124	0.1121	0.1119	-0.18
2	6.4042	0.0306	0.0308	0.0307	0.0307	0.0306	-0.33
3	9.0519	0.0230	0.0231	0.0231	0.0230	0.0229	-0.43
4	9.9315	0.0122	0.0123	0.0124	0.0123	0.0123	0.0
5	30.3133	0.0483	0.0524	0.0561	0.0498	0.0499	0.20

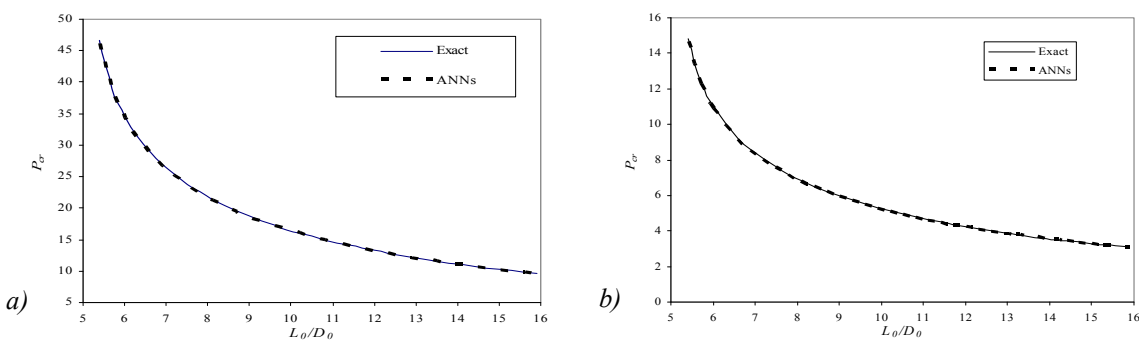

Fig. 6. *Dimensional critical buckling loads (in Newtons) for n = 17, d = 1 mm, E = 206 Gpa with a) The spring index, C =6.5, b) The spring index, C =11.5*

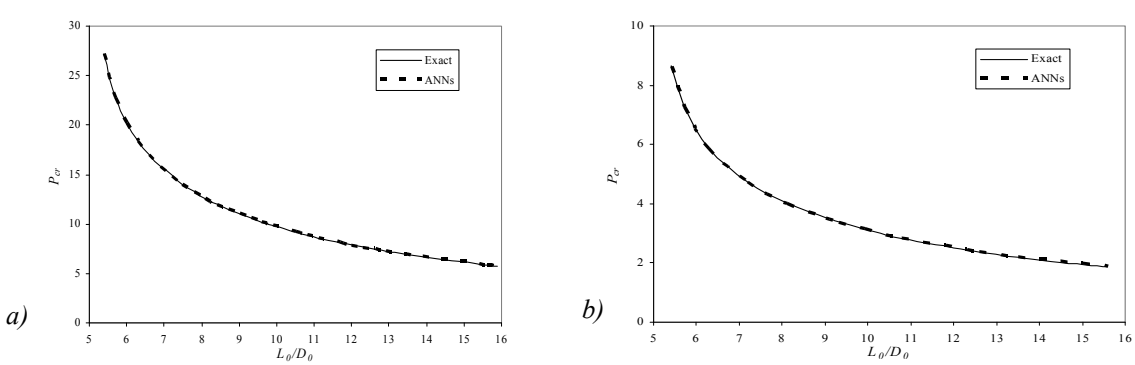

Fig. 7. *Dimensional critical buckling loads (in Newtons) for n = 29, d = 1 mm, E = 206 Gpa Gpa with a) The spring index, C =6.5, b) The spring index, C =11.5*

For the best estimation of the critical buckling loads a three layer – BP algorithm is used with a training data set which consisted of 3662 patterns which are obtained from the exact numerical solution of the differential equation set which governs the buckling behavior of helical springs and given by Eq. (7). The questioning set with 1305 patterns gives distinct errors of a maximum of 0.93%. Hence, almost perfect weight values are obtained to predict the non-dimensional buckling loads.

Since there is no analytical expression for the critical buckling loads for the helical compression springs with rectangle or hollow sections, the proposed ANN method may be used as a quick estimate of these loads in the design stage based on the theory presented in this work. Finally, for the design of compression helical springs with different sections and shapes it is possible that an extensive software package based on the ANN is developed by considering static, buckling and vibration states.

ACKNOWLEDGEMENT

The material covered in this paper is based upon work which was supported by the research grant 106M307 from Technical Research Council of Turkey (TUBITAK).

7 REFERENCES

[1] Haringx, J.A. (1949). On highly compressible helical springs and rubber rods. and their application for vibration-free mountings. *Philips Research Reports*, vol. 4, p. 49-80.

[2] Tabarrok, B., Xiong, Y. (1989). On the buckling equations for spatial rods. *Int. J. of Mech.Eng. Sci,* vol. 31 no. 3, p. 179-192.

[3] Tabarrok, B., Xiong, Y. (1992). A spatially curved and twisted rod element for buckling analysis. *Int.ernational Journal of Solids and Structures*, vol. 29, no. 23, p. 3011-3023.

[4] Xiong, Y., Tabarrok, B. (1992). A finite element model for the vibration of spatial rods under various applied loads. *Int. J. of Mech. Eng. Sci.*, vol. 34, no. 1, p. 41-51.

[5] Pearson, D. (1982). The transfer matrix method for the vibration of compressed helical springs. *J. of Mech. Eng. Sci.,* vol. 24, p. 163-171.

[6] Haktanır, V. (1990). *The investigation of the statical. dynamic and buckling behavior of helical rods by the transfer and stiffness matrices methods.* Ph.D. Thesis. Çukurova University. Mechanical Engineering Department (In Turkish).

[7] Becker, L.E., Cleghorn, W.L. (1992). On the buckling of helical compression springs. *Int. J. of Mech. Eng. Sci.*, vol. 34, no. 4, p. 275-282.

[8] Becker, L.E., Cleghorn, W.L. (1994). The buckling behavior of rectangular-bar helical compression springs. *Journal of Applied Mechanics,* vol. 61, p. 491-493.

[9] Chassie, G.G., Becker, L.E., Cleghorn, W.L. (1997). On the buckling of helical springs under combined compression and torsion. *International Journal of Mechanical Sciences,* vol. 39, no. 6, p. 697-704.

[10] Yıldırım V., Tütüncü N., İbrikçi T. (2009). *TUBITAK Technical Final Report* for the grant 106M307.

[11] Yıldırım, V. (1999). An efficient numerical method for predicting the natural frequencies of cylindrical helical springs. *Int. J. of Mech.Eng. Sci.*, vol. 41, no. 8, p. 919-939.

[12] Ibrikci, T. (2000). *Neural networks models for protein structure prediction*. *PhD. Thesis*, Cukurova University.

[13] Rumelhart, D.E., Hinton, G.E. ,Williams, R.J. (1986). Learning internal representations by error propagation in parallel distributed processing: *Explorations in the microstructure of Cognition* MIT Press, p. 318-362

[14] Alpaydin, E. (2004). *Introduction to Machine Learning*, MIT Press, USA.

[15] Hsu, Y.L., Wang, S.G., Yu, C.C. (2003). A sequential approximation method using neural networks for engineering design optimization problems. *Engineering Optimization*, vol. 35, no. 5, p. 489-511.

[16] The MathWorks Inc. (2006). *Matlab Help* 1984-2006.